Inorganic Chemistry

Article

pubs.acs.org/IC

Linear and T-Shaped Iron(I) Complexes Supported by N-Heterocyclic Carbene Ligands: Synthesis and Structure Characterization

Zhenwu Ouyang,[†] Jingzhen Du,[†] Lei Wang,[†] Jared L. Kneebone,[‡] Michael L. Neidig,[‡] and Liang Deng*[,†]

[†]State Key Laboratory of Organometallic Chemistry, Shanghai Institute of Organic Chemistry, Chinese Academy of Sciences, 345 Lingling Road, Shanghai 200032, China

[‡]Department of Chemistry, University of Rochester, New York 14627, United States

Supporting Information

ABSTRACT: The use of the N-heterocyclic carbene (NHC) ligands 1,3-bis(2′,6′-diethylphenyl)-4,5-$(CH_2)_4$-imidazol-2-ylidene (cyIDep), 1,3-bis(2′,6′-diethylphenyl)-imidazolin-2-ylidene (sIDep), and its N-mesityl analogue sIMes enables the preparation of the two-coordinate homoleptic iron(I)-NHC complexes $[(cyIDep)_2Fe][BAr^F{}_4]$ (**3**, Ar^F denoted for 3,5-di(trifluoromethyl)phenyl) and $[(sIDep)_2Fe][BAr^F{}_4]$ (**4**) and the T-shaped iron(I)-NHC complex $[(sIMes)_2Fe(THF)][BPh_4]$ (**5**, THF = tetrahydrofuran). Complexes **3**−**5** were prepared via the sequential protocol of control reduction of iron(II) dihalides by KC_8 in the presence of the corresponding NHC ligands followed by halide-abstraction with $NaBAr_4$. Spectroscopic characterization, including single-crystal X-ray diffraction studies and ^{57}Fe Mössbauer spectroscopy, in combination with density functional theory calculations, suggest their high-spin nature. Solution property study (absorption spectroscopy and cyclic voltammetry) indicates that **3** and **5** keep their corresponding two- and three-coordinate nature in THF solution, and **4** might reversibly coordinate a THF molecule to form, presumably, the T-shaped species $[(sIDep)_2Fe(THF)][BAr^F{}_4]$. The isolation of **3** and **4** demonstrates the accessibility of homoleptic two-coordinate iron(I)-NHC complexes.

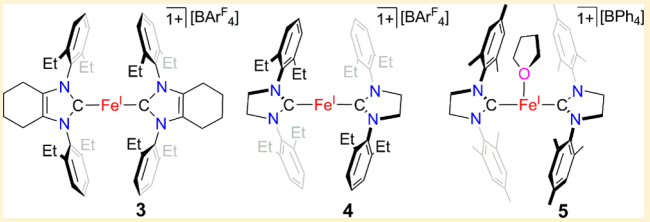

INTRODUCTION

Low-coordinate iron(I) complexes (e.g., coordination numbers (CNs) of 3 and 2) are distinctive as iron(I) is an uncommon oxidation state and CNs less than 4 are rare for iron.[1,2] The coexistence of these unusual structure features renders the synthesis of low-coordinate iron(I) complexes challenging as this type of species could have the tendency not only to undergo disproportionation but also to coordinate with exogenous ligands. Their promising chemical and physical properties, for example, small molecule activation[3] and single-molecule magnet behavior,[4] however, have stimulated significant synthetic efforts in the recent years.

The stabilization of low-coordinate iron(I) complexes necessitates bulky supporting ligands. So far, bidentate β-diketiminate ligands bearing bulky N-aryl substituents proved privileged in stabilizing three-coordinate iron(I) complexes. Holland, as the pioneer in this area, achieved the syntheses of three-coordinate β-diketiminate iron(I) complexes with hydride,[5] sulfide,[6] alkenes,[7] and alkynes[7] as coligands. Some of the β-diketiminate iron(I) species can activate N_2.[3a,8] In addition to the β-diketiminate iron(I) complexes, Caulton reported a unique T-shaped iron(I) complex $[(({}^tBu_2PCH_2SiMe_2)_2N)Fe]$,[9] and Jones reported a dinuclear iron(I) guanidinate compound $[(DippN)_2C(cis\text{-}2,6\text{-}Me_2NC_5H_8)Fe]_2$ (Dipp = 2,6-diisopropylphenyl) that contains an Fe−Fe bond.[10] Two-coordinate iron(I) complexes have remained unknown until Long's first report on $[K(crypt\text{-}222)][Fe(C(SiMe_3)_3)_2]$ in 2013.[11] Until now, several two-coordinate iron(I) complexes have been reported (Chart 1).[12−17] In these two-coordinate iron(I) complexes, bulky anionic ligands, such as $[C(SiMe_3)_3]^{1-}$, $[NSiMe_3(Dipp)]^{1-}$, and $[N(SiMe_3)_2]^{1-}$, and neutral carbene ligands, imidazol-2-ylidenes, cyclic alkylaminocarbenes (cAACs),[18] are utilized. A notable property of these two-coordinate complexes is slow magnetic relaxation behavior typical of single-molecule magnets.[11,13,16]

Chart 1. Reported Two-Coordinate Iron(I) Complexes

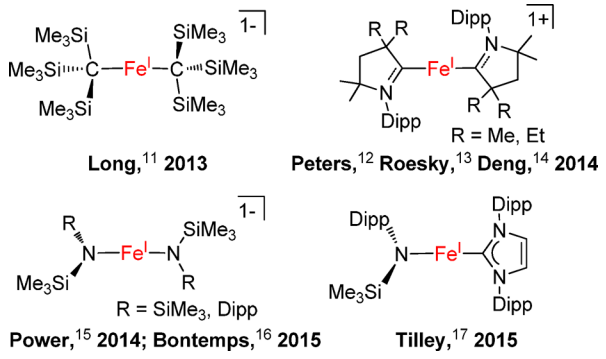

Received: July 8, 2015
Published: August 14, 2015

DOI: 10.1021/acs.inorgchem.5b01522
Inorg. Chem. 2015, 54, 8808−8816

Different from cAACs that are good π-accepting ligands, imidazol-2-ylidenes, the more common N-heterocyclic carbene (NHC) ligands, are thought to be good σ-donating ligands with a weak but variable π-accepting ability.[18b,19] Recently, we and others found that monodentate imidazol-2-ylidenes can serve as supporting ligands for low-coordinate iron(II)[20] and iron(IV)[21] complexes. With olefins as coligands, the low-coordinate iron(0)-NHC complex, for example, [(IMes)Fe(η^2:η^2-dvtms)] (dvtms = divinyltetramethyldisiloxane), is also accessible.[21] Regarding these, limited progress has been made on the synthesis of low-coordinate iron(I)-NHC complexes. We found that the one-electron reduction reaction of [$(IMes)_2FeCl_2$] (IMes: 1,3-dimesitylimidazol-2-ylidene) by sodium amalgam can furnish a three-coordinate iron(I) complex [$(IMes)_2FeCl$], which readily disproportionates in solution to a mixture of iron(0) and iron(II) species.[14] The attempts to prepare the two-coordinate species $[(IMes)_2Fe]^+$ from [$(IMes)_2FeCl$] by chloride-abstraction with $NaBAr_4$ were unsuccessful.[14] On the other hand, Tilley and his co-workers achieved the synthesis of the first heteroleptic two-coordinate iron(I) complex bearing an imidazol-2-ylidene ligand, [(IPr)Fe($NDippSiMe_3$)] (IPr: 1,3-bis(2′,6′-diisopropylphenyl)imidazol-2-ylidene) using the two-coordinate iron(II) complex [$Fe(NDippSiMe_3)_2$] as the iron precursor.[17] The attainment of [(IPr)Fe($NDippSiMe_3$)], thus, hints the accessibility of the homoleptic two-coordinate iron(I)-imidazol-2-ylidene complexes. Inspired by these, we then targeted NHCs with more steric hindrance and/or less steric flexibility over IMes as supporting ligands. We report herein the preparation and characterization of the first homoleptic two-coordinate iron(I)-NHC complexes and a three-coordinate T-shaped iron(I) complex with the six-membered ring-fused imidazol-2-ylidene and imidazolin-2-ylidenes as supporting ligands (Chart 2).

Chart 2. Designations for NHC Ligands and Iron(I)-NHC Complexes

Three-Coordinate		*Two-Coordinate*	
[$(cyIDep)_2FeBr$]	(1)	[$(cyIDep)_2Fe][BAr^F_4$]	(3)
[$(sIDep)_2FeBr$]	(2)	[$(sIDep)_2Fe][BAr^F_4$]	(4)
[$(sIMes)_2Fe(THF)][BPh_4$]	(5)		

cyIDep

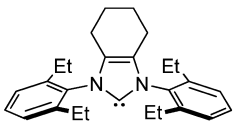

sIDep

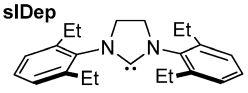

sIMes

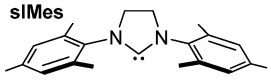

RESULTS AND DISCUSSION

Synthesis and Characterization of Three-Coordinate NHC-Iron(I) Bromides. Following the synthetic route for [$(IMes)_2FeCl$],[14] we examined the reduction reactions of ferrous halides with KC_8 in the presence of a variety of NHCs and successfully prepared two new three-coordinate iron(I)-NHC complexes (**1** and **2**).

The addition of an excessive amount of KC_8 (2.5 equiv) to a preformed mixture of $FeBr_2$ with 1,3-bis(2′,6′-diethylphenyl)-4,5-$(CH_2)_4$-imidazol-2-ylidene (cyIDep, 2 equiv) or 1,3-bis-(2′,6′-diethylphenyl)-imidazolin-2-ylidene (sIDep, 2 equiv) in toluene produced a brown or purple suspension, from which the iron(I)-NHC complex [$(cyIDep)_2FeBr$] (**1**) or [$(sIDep)_2$-FeBr] (**2**) was isolated as brown or purple solid, respectively, in good yields (Scheme 1). Attempts to access similar iron(I)

Scheme 1. Preparation Route for 1 and 2

$FeBr_2$ —(+ 2 cyIDep or sIDep, THF)→ —(x.s. KC_8, toluene)→ [$(cyIDep)_2FeBr$] (**1**) yield: 64% or [$(sIDep)_2FeBr$] (**2**) yield: 82%

halide complexes using 1,3-bis(2′,6′-diisopropylphenyl)-imidazol-2-ylidene (IPr), 1,3-diadamantylimidazol-2-ylidene (IAd), and 1,3-di-*tert*-butylimidazol-2-ylidene (I^tBu) as the ancillary ligands were unsuccessful. In these cases, while homogeneous solution could be formed when mixing the ferrous salt with 2 equiv of the NHC ligands, the further interaction of the mixture with KC_8 led to the formation of iron black and free NHCs. Noting the similar electronic properties of these NHCs,[18b] the different outcome indicated the selection of NHCs with appropriate steric properties is crucial for the preparation of low-coordinate iron(I)-NHC halides.

Complexes **1** and **2** are air- and moisture-sensitive. Under N_2 atmosphere, they decompose slowly in solution (C_6H_6 and tetrahydrofuran (THF)) with the formation of black precipitates and free NHCs (as revealed by ^1H NMR spectroscopy). In the solid state, they can be kept for weeks at −25 °C without noticeable decomposition. X-ray crystallographic studies established the molecular structures of **1** and **2** as trigonal planar iron(I) complexes (Figure 1). Table 1 lists their key

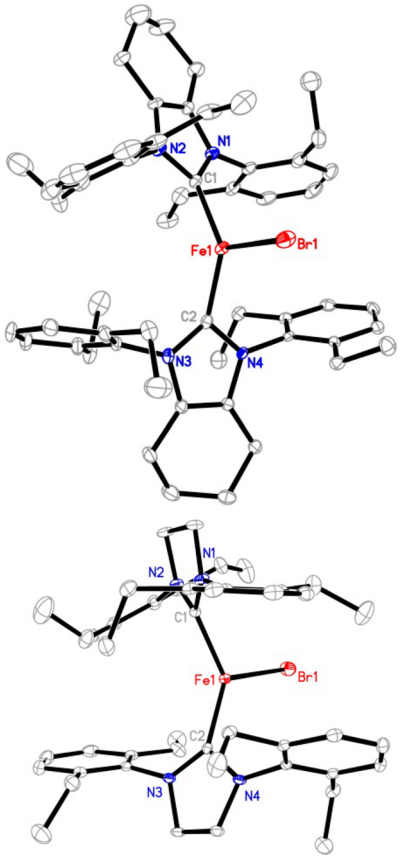

Figure 1. Molecular structures of **1** (upper, showing one of the two crystallographically independent molecules in the unit cell) and **2** (lower) with 30% probability ellipsoids. Hydrogen atoms are omitted for clarity.

DOI: 10.1021/acs.inorgchem.5b01522
Inorg. Chem. 2015, 54, 8808−8816

Table 1. Selected Bond Lengths and Angles of 1−5, [(IMes)$_2$FeCl] (6), and [(Me$_2$-cAAC)$_2$Fe][BAr$^F_4$] (7) from X-ray Diffraction Studies, and their ^{57}Fe Mössbauer Spectroscopic Data

	1[a]	2	3[a]	4	5	6[b]	7[b]
Fe−C (Å)	2.023(4)	2.013(3), 2.020(3)	1.996(7)	1.983(5), 1.971(5)	1.989(5), 1.972(5)	1.998(9), 2.030(8)	1.997(3), 1.997(3)
Fe−X (Å)[c]	2.402(1)	2.387(1)			2.145(3)	2.258(3)	
C−N (Å)[d]	1.373(5)	1.353(3) to 1.362(3)	1.359(8)	1.333(6) to 1.351(6)	1.347(6) to 1.357(6)	1.349(13) to 1.404(11)	1.310(3)
C−Fe−C (deg)	133.3(1)	130.6(1)	178.4(3)	175.8(2)	162.9(1)	125.6(3)	180
C−Fe−X (deg)[c]	113.3(1)	109.9(1), 119.5(1)			95.0(1), 102.1(1)	116.4(3), 118.0(3)	
δ (mm/s)	0.69	0.65	0.48	0.55	0.65	0.65	0.49
ΔE_Q (mm/s)	2.36	2.27	5.75	6.82	5.99	2.63	4.58

[a]Structure data are the average of two crystallographically independent molecules in the unit cell. [b]Data from ref 14. [c]X = Br for **1** and **2**, O for **5**, Cl for **6**. [d]Range of the C(carbene)−N distances.

structural parameters in addition to those of [(IMes)$_2$FeCl] for comparison.[14] In spite of the difference of the ligands, the Fe−C(carbene) distances in these three-coordinate iron(I)-NHC halide complexes are all ∼2.00 Å, and their C(carbene)−Fe−C(carbene) angles span a narrow range (125.6(3) to 133.3(1)°). The angles are much smaller than those (166.4(1) to 168.3(1)°) of the congeners of the T-shaped nickel complexes [(NHC)$_2$NiX] (NHC = IMes, X = Cl, Br, I; NHC = IPr, X = Cl).[22] The larger atomic radius of iron over nickel, which renders long M−C(carbene) bonds and less severed steric repulsion between the NHCs in the iron complexes, could be one of the causes leading to the structure difference between the iron(I) and nickel(I) complexes. The quadrupole doublets in the 80 K Mössbauer spectra of **1** and **2** (Figures S1 and S2) have comparable isomer shifts (δ = 0.69 and 0.65 mm/s, respectively) and quadrupole splittings (ΔE_Q = 2.36 and 2.27 mm/s), similar to the parameters previously reported for [(IMes)$_2$FeCl] (δ = 0.65 mm/s, ΔE_Q = 2.63 mm/s).[14] These parameters are in agreement with the parameters expected for high-spin three-coordinate iron(I) complexes.

Synthesis and Characterization of Two-Coordinate Iron(I)-NHC Complexes. The 2,6-diethylphenyl (Dep)-substituted NHC complexes, **1** and **2**, proved to be effective precursors for the synthesis of two-coordinate iron(I)-NHC complexes. The interaction of **1** or **2** with 1 equiv of NaBAr$^F_4$ in Et$_2$O led to the formation of a red or orange solution, respectively. After further workup and recrystallization, red purple crystals of [(cyIDep)$_2$Fe][BAr$^F_4$] (**3**) and orange crystals of [(sIDep)$_2$Fe][BAr$^F_4$] (**4**) were isolated in 80% and 65% yields, respectively (Scheme 2). Complexes **3** and **4** were

Scheme 2. Preparation Route for 3 and 4

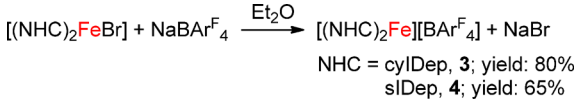

characterized by ^{1}H NMR spectroscopy, solution magnetic susceptibility measurement, UV−vis−NIR spectroscopy, X-ray crystallography, ^{57}Fe Mössbauer spectroscopy, and elemental analysis. They are air- and moisture-sensitive, soluble in Et$_2$O and THF, and insoluble in toluene and *n*-hexane.

Complexes **3** and **4** represent rare two-coordinate homoleptic iron-NHC complexes. Transition metal imidazol-2-ylidene complexes in the form of [(NHC)$_2$M]^n are well-known for groups 10 and 11 metals (Ni,[23] Pd,[24] Pt,[25] Cu,[26] Ag,[27] Au[28]). For the earlier transition metals, only the cobalt complex [(IMes)$_2$Co][BPh$_4$] was reported by us.[29] Table 1 lists the key structural parameters of **3** and **4** obtained from single-crystal X-ray diffraction studies. The structures of the cations in **3** and **4** are shown in Figure 2. Similar to their group 9−11

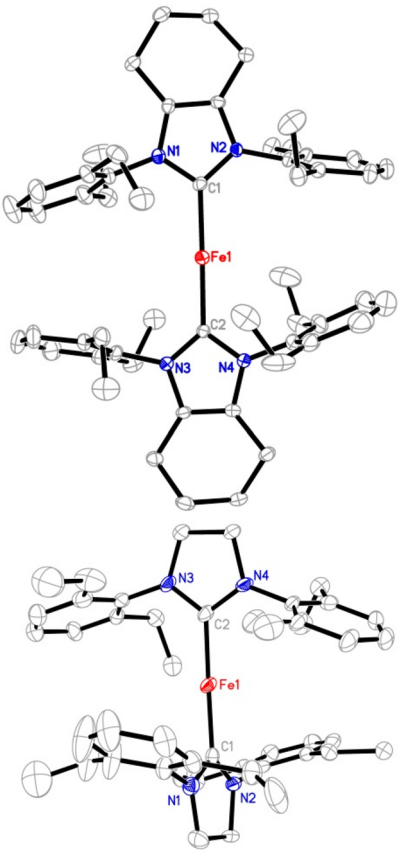

Figure 2. Structures of the cationic part of **3** (top, showing one of the two crystallographically independent cations in the unit cell) and **4** (bottom) showing 30% probability ellipsoids. Hydrogen atoms are omitted for clarity.

metal analogues,[23−29] the C−Fe−C cores in **3** and **4** show a linear alignment (178.4(3)° and 175.8(2)°). The Fe−C distances in **3** and **4** (1.996(7) and 1.977(5) Å in average, respectively) are longer than those of their group 9−11 analogues, for example, 1.937(3) Å in [(IMes)$_2$Co]$^+$,[29] 1.940(3) Å in [(6-Mes)$_2$Ni]$^+$,[23] and 1.871(3) Å in [(IMes)$_2$Cu]$^+$,[26] consistent with the larger atomic radius of iron versus the other later 3d metals. The two imidazole planes in **3** form a small dihedral angle of 24.2(1)°, whereas a large dihedral angle of 70.4(1)° between the two planes is observed in **4**. The different dihedral angles might be due to crystal

DOI: 10.1021/acs.inorgchem.5b01522
Inorg. Chem. 2015, 54, 8808−8816

packing forces, suggesting the free rotation of the NHC ligands along the Fe−C(carbene) axis in $[(cyIDep)_2Fe]^+$ and $[(sIDep)_2Fe]^+$ in solution. In addition, the eight ethyl groups on the Dep moieties in both complexes align randomly, and no short contact between the N-Dep groups and the iron center was observed.

The 80 K ^{57}Fe Mössbauer spectra of **3** and **4** feature quadrupole doublets (Figure 3). Their isomer shifts (0.48 and 0.55 mm/s for **3** and **4**, respectively), being negatively shifted by ca. 0.20 and 0.10 mm/s versus those of the corresponding iron(I) bromide complexes **1** and **2**, are comparable to that of the linear iron(I)-cAAC complex $[(Me_2\text{-cAAC})_2Fe][BAr^F{}_4]$ (0.49 mm/s).[14] The fitting quadrupole splitting values from the spectra of **3** and **4** are very large (5.75 and 6.82 mm/s, respectively). To our knowledge, the latter value is the largest quadrupole splitting ever observed in iron complexes. Precedents of iron complexes with quadrupole splittings larger than 5 mm/s are known for high-valent iron nitride complexes supported by tripodal ligands and low-valent iron−chromium complexes supported by double-decker ligands.[30] While the causes leading to these large quadrupole splittings of **3** and **4** need further detailed electronic structure studies, we noted that $[(Me_2\text{-cAAC})_2Fe][BAr^F{}_4]$ also has a large quadrupole splitting of 4.58 mm/s, and speculated that the asymmetric electron distribution around the iron centers caused by the diagonal NHC ligand fields might be one of causes.[30d,31] Lastly, the broadness observed in the doublet of **4** likely represents small variations in bond distances and angles of this complex in the solid-state powder.

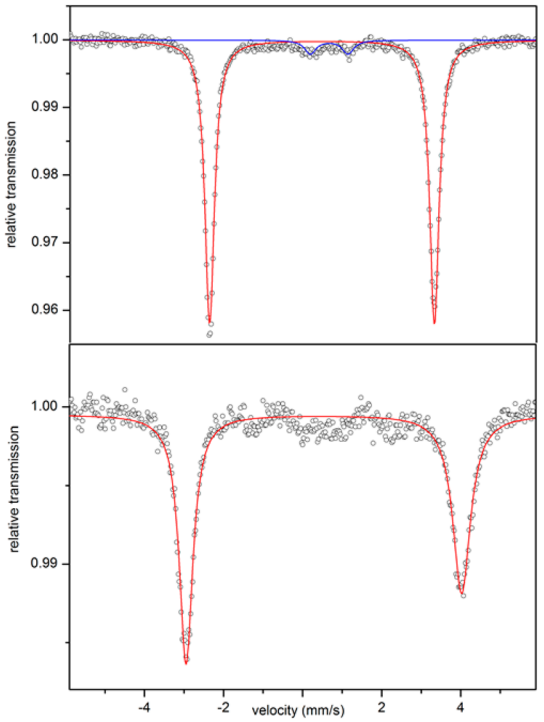

Figure 3. 80 K ^{57}Fe Mössbauer spectra of $[(cyIDep)_2Fe][BAr^F{}_4]$ (**3**, upper) and $[(sIDep)_2Fe][BAr^F{}_4]$ (**4**, lower) measured under a 0.07 T applied magnetic field. The data (dots) and fits (solid lines, red for the major species) are shown. For the spectrum of **3**: the parameters of the major species (red line, ∼95% of iron) are given in the main text (Table 1). A minor species (blue line, ∼5% of iron with δ = 0.66 mm/s and ΔE_Q = 0.95 mm/s) is also present. Because of the low intensity, no attempts to fit impurities in the spectrum of **4** were made.

The ^{1}H NMR spectra of **3** and **4** measured in THF-d_8 exhibited six (20.67, 17.94, 15.53, 4.00, 3.52, −10.83 ppm) and five (21.70, 18.65, 4.41, 3.19, −78.38 ppm) paramagnetically shifted peaks corresponding to the signals of cyIDep and sIDep ligands, respectively. In addition to these, signals of free sIDep were observed in the spectrum of **4**, and their intensity increased after standing in solution for days, whereas no resonances responsible for free cyIDep were noticed in the spectrum of **3** after standing in solution at room temperature for one week. While single-point calculations on the cations in **3** and **4** at their doublet and quartet states based on the molecular structures revealed by XRD indicated a quartet state (S = 3/2) as their common ground state (Table s2), the measured solution magnetic moment for **3** (5.5(2) μB) in THF is larger than the spin-only value (3.8 μB) of S = 3/2 ions, likely due to unquenched orbital momentum contribution as observed in $[(DippNC^tBu)_2CH)Fe(\eta^2\text{-HCCPh})]$ (4.7 μB).[32] The proneness of **4** to coordinate with THF prevents solution magnetic susceptibility measurement (vide infra).

When dissolved in THF, both the solutions of **3** and **4** exhibit red color. However, their absorption spectra in the NIR region are distinct. The spectrum of **3** shows four clear NIR bands around 746, 835, 1310, and 1419 nm with extinction coefficients of ∼100 M^{-1} cm^{-1} (Figure 4). These bands are tentatively assigned to ligand-field transitions of two-coordinate d^7 iron(I) center[2d] and are consistent with the four-band-pattern observed in the NIR absorption spectrum of the two-coordinate d^7 cobalt(II) species $[Co(N(SiMe_3)_2)_2]$.[33] When recorded in Et_2O, the absorption spectrum of **3** is nearly identical to that measured in THF. In contrast, the spectrum of **4** measured in THF features three heavily broadened NIR absorption bands at 780, 1150, and 1350 nm, and four NIR bands at 706, 791, 1192, and 1352 nm were observed when recorded in Et_2O (black lines in Figure 4). These observations suggest that **4** might bind reversibly with THF to form $[(sIDep)_2Fe(THF)][BAr^F{}_4]$ and that **3** is inert toward THF. The difference is probably related to higher steric flexibility of sIDep over cyIDep, which enables the cation $[(sIDep)_2Fe]^+$ to coordinate THF upon twisting the arrangement of the N-Dep groups toward the imidazole plane. Accordingly, we reason that the measured ^{1}H NMR spectrum of **4** in THF should be

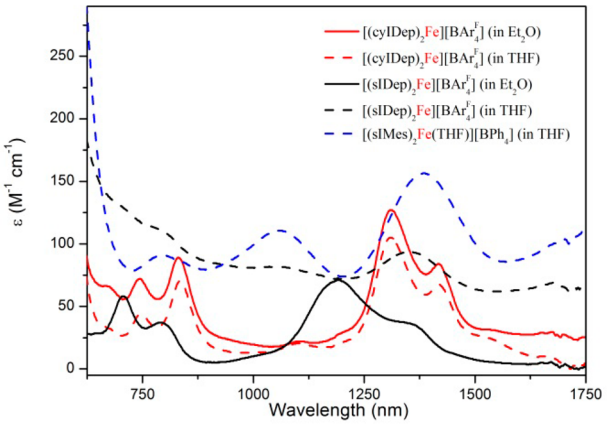

Figure 4. Absorption spectra of $[(cyIDep)_2Fe][BAr^F{}_4]$ (**3**, red lines), $[(sIDep)_2Fe][BAr^F{}_4]$ (**4**, black lines), and $[(sIMes)_2Fe(THF)][BAr^F{}_4]$ (**5**, blue line) in NIR region measured at room temperature.

DOI: 10.1021/acs.inorgchem.5b01522
Inorg. Chem. 2015, 54, 8808−8816

corresponding to the mixture of $[(sIDep)_2Fe][BAr^F_4]$ and $[(sIDep)_2Fe(THF)][BAr^F_4]$.

Synthesis and Characterization of T-Shaped Iron(I)-NHC Complex. The different NIR absorptions of **4** in THF and Et_2O prompted attempts to isolate $[(sIDep)_2Fe(THF)][BAr_4]$, which, however, were unsuccessful likely due to the ease of the species to lose THF. Considering this, efforts to access the analogous complex $[(sIMes)_2Fe(THF)][BAr_4]$, bearing the less sterically demanding NHC ligand sIMes, were pursued. The preparation of $(sIMes)_2FeCl$ following a similar protocol to that previously employed for the preparation of $[(sIDep)_2FeBr]$ (**2**) was frustrated by the readily disproportionation reaction of this species in solution. However, the one-pot reaction protocol shown in Scheme 3 eventually enabled the preparation of $[(sIMes)_2Fe(THF)][BPh_4]$ (**5**) as a red crystalline solid in the form of **5**·Et_2O in 44% isolated yield.

Scheme 3. Preparation Route for 5

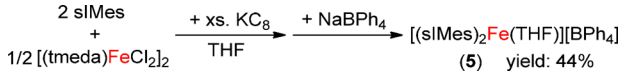

A single-crystal X-ray diffraction study established the structure of the cation in **5** as a T-shaped iron(I) species with two sIMes ligands on the axial positions and a coordinated THF molecule on the equatorial site (Figure 5). The

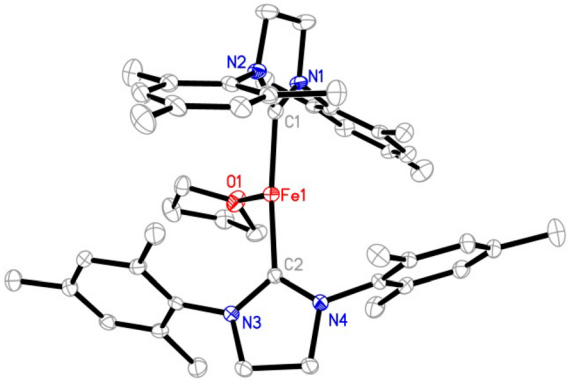

Figure 5. Structure of the cation in **5** showing 30% probability ellipsoids. Hydrogen atoms are omitted for clarity.

C(carbene)−Fe−C(carbene) angle in $[(sIMes)_2Fe(THF)]^+$ (162.9(1)°) is intermediate between those of the two-coordinate species $[(sIDep)_2Fe]^+$ (175.8(2)°) and the trigonal planar complex $[(sIDep)_2FeBr]$ (130.6(1)°). Its Fe−C(carbene) bond length (average of 1.980(5) Å) and the dihedral angle between the two imidazole planes (82.9(1)°) are close to the corresponding ones in $[(sIDep)_2Fe]^+$. The long Fe−O distance (2.145(3) Å), compared to that in $[(nacnac)Fe(OEt_2)][BAr^F_4]$ (1.978(4) Å),[34] indicates the lability of the coordinated THF molecule. The Mössbauer isomer shift (0.65 mm/s) observed from the spectrum of **5** (Figure 6) is comparable to those of trigonal-planar species **1** and **2**; meanwhile, the quadrupole splitting (5.99 mm/s) is close to those of the two-coordinate iron(I)-NHC complexes **3** and **4**. The broadness observed in the doublet of **5** likely represents small variations in bond distances and angles of this complex in the solid-state powder. The Mössbauer data are suggestive of an iron(I) nature for **5**.

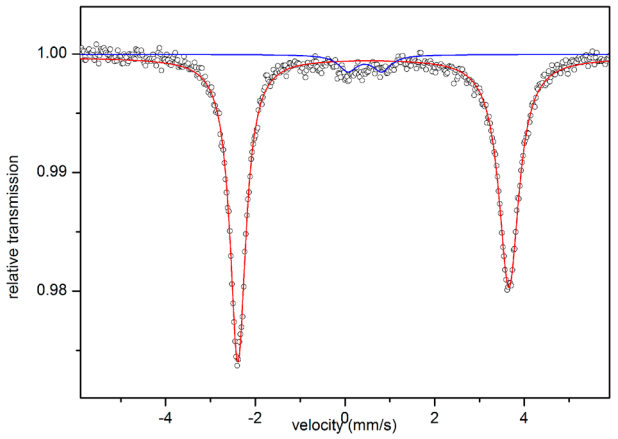

Figure 6. 80 K ^{57}Fe Mössbauer spectrum of $[(sIMes)_2Fe(THF)][BPh_4]$ (**5**) measured under a 0.07 T applied magnetic field. The data (dots) and fits (solid lines, red for the major species) are shown. The parameters of the major species (red line, ∼93% of iron) are given in the main text (Table 1). A minor species (blue line, ∼7% of iron with δ = 0.44 mm/s and ΔE_Q = 0.75 mm/s) is also present.

The solution properties of **5** proved similar to that of **4** in THF. The ^{1}H NMR spectrum of **5** in THF-d_8 shows four paramagnetically shifted resonances at 7.97, 2.47, 1.88, and −71.26 ppm. Its absorption spectrum in THF displays three clear NIR bands at 796, 1060, and 1386 nm (Figure 4). The wavelengths of these maximum absorptions resemble those of **4** in THF. Moreover, cyclic voltammetry studies on the solutions of **4** and **5** revealed quasi-reversible redox waves with large peak-to-peak separation (0.58 and 0.20 V, respectively; Figure S6), assignable to the redox processes of $[(NHC)_2Fe(THF)]^{1+/2+}$. In contrast, the voltammogram of **3** features an irreversible oxidation wave with the peak potential of −0.38 V (Figure S7), suggesting the inability of the bis(cyIDep) ligand field to stabilize iron(II) species. Despite the aforementioned similarities, **5** is found more stable than **4**, as the THF solution of **5** can be kept at room temperature for days with negligible decomposition.

CONCLUSIONS

In this study, we have achieved the preparation and characterization of a series of three- and two-coordinate iron(I) complexes with NHCs as supporting ligands. Further studies on the magnetic properties and electronic structures of these low-coordinate iron(I)-NHC complexes are ongoing. The following are the principle findings of this study.

(1) Two NHC ligands, namely, cyIDep and sIDep, were found effective supporting ligands for two-coordinate homoleptic iron(I)-NHC complexes. The one-pot reaction protocol of treating $FeBr_2$ with 2 equiv of cyIDep and sIDep followed by controlled reduction with excess amounts of KC_8 enables the preparation of the three-coordinate iron(I)-NHC complexes $[(cyIDep)_2FeBr]$ (**1**) and $[(sIDep)_2FeBr]$ (**2**). The further salt elimination reactions of **1** and **2** with $NaBAr^F_4$ in Et_2O led to the preparation of the rare two-coordinate homoleptic iron(I)-NHC complexes $[(cyIDep)_2Fe][BAr^F_4]$ (**3**) and $[(sIDep)_2Fe][BAr^F_4]$ (**4**), respectively. Complexes **1**−**4** were characterized by various spectroscopic methods including single-crystal X-ray diffraction and ^{57}Fe Mössbauer spectroscopy, which indicate their

DOI: 10.1021/acs.inorgchem.5b01522
Inorg. Chem. 2015, 54, 8808−8816

high-spin nature. The attainment of the two-coordinate iron(I)-NHC complexes indicates the importance of suitable steric protection conferred by the N-substituents on the NHC ligands for the stabilization of low-coordinate iron(I)-NHC complexes.

(2) The unique T-shaped iron(I)-NHC complex $[(sIMes)_2Fe(THF)][BPh_4]$ (**5**) was prepared and fully characterized by various spectroscopic methods. Solution property studies on **3**−**5** by ^{1}H NMR and UV−vis−NIR spectroscopies indicate that **3** and **5** keep their two-coordinate and T-shaped nature, respectively, in solution phase, and that the cation in **4** reversibly coordinates a THF molecule to form T-shaped species $[(sIDep)_2Fe(THF)]^+$. Cyclic voltammetry studies reveal a quasi-reversible one-electron redox wave for the three-coordinate species $[(NHC)_2Fe(THF)]^{1+/2+}$ (NHC = sIMes and sIDep) in THF. In contrast, the voltammogram of the two-coordinate complex **3** only exhibited an irreversible oxidation wave. The different solution properties of **3**−**5** might result from the less steric flexibility of cyIDep, which is enforced by the presence of 4,5-subsitutents on the carbene ligand, over sIDep and sIMes.

EXPERIMENTAL SECTION

General Procedures. All experiments referring to NHCs or iron complexes were performed either under an atmosphere of dry dinitrogen with the rigid exclusion of air and moisture using standard Schlenk techniques or in a glovebox. Organic solvents were dried with a solvent purification system (Innovative Technology) and bubbled with dry N_2 gas prior to use. ^{1}H NMR, ^{13}C NMR, ^{11}B{^{1}H}, and ^{19}F NMR spectra were recorded on an Agilent 300, 400, or 600 MHz spectrometer. All chemical shifts were reported in units with references to the residual protons of the deuterated solvents for proton and carbon chemical shifts, and to external CF_3COOH (0.00 ppm) for fluoro chemical shifts. Elemental analysis was performed by the Analytical Laboratory of Shanghai Institute of Organic Chemistry (CAS). Magnetic moments were measured by the method originally described by Evans with stock and experimental solutions containing a known amount of a $(CH_3)_3SiOSi(CH_3)_3$ standard.[35] Absorption spectra were recorded with a Shimadzu UV-3600 UV−vis−NIR spectrophotometer. Cyclic voltammetry measurements were made with a CHI 600D potentiostat in THF solutions using a sweep rate of 100 mV/s, a glassy-carbon working electrode, 0.05 M $[Bu^n_4N][BPh_4]$ supporting electrolyte, and a saturated calomel electrode as reference electrode. Under these conditions, $E_{1/2}$ = 0.55 V for the $[Cp_2Fe]^{0/+}$ couple.

X-ray Structure Determination. Diffraction-quality crystals were obtained as **1**−**4** and **5**·Et_2O from recrystallizations in toluene/*n*-hexane, Et_2O, Et_2O/*n*-hexane, and THF/Et_2O, respectively, at −25 °C. Crystals were coated with mineral oil and mounted on a Bruker APEX CCD-based diffractometer equipped with an Oxford low-temperature apparatus. Data were collected at 130(2) K. Cell parameters were retrieved with SMART software and refined using SAINT software on all reflections. Data integration was performed with SAINT, which corrects for Lorentz polarization and decay. Absorption corrections were applied using SADABS.[36] Space groups were assigned unambiguously by analysis of symmetry and systematic absences determined by XPREP. All structures were solved and refined using SHELXTL.[37] Metal and first coordination sphere atoms were located from direct-methods E-maps. Non-hydrogen atoms were found in alternating difference Fourier synthesis and least-squares refinement cycles and during final cycles were refined anisotropically. Table S1 summarizes the crystal data and summary of data collection and refinement for the complexes.

^{57}Fe Mössbauer Spectroscopy. All solid samples for ^{57}Fe Mössbauer spectroscopy were run on nonenriched samples of the as-isolated complexes. Each sample was loaded into a Delrin Mössbauer sample cup for measurements and loaded under liquid nitrogen. Low-temperature ^{57}Fe Mössbauer measurements were performed using a See Co. MS4 Mössbauer spectrometer integrated with a Janis SVT-400T He/N_2 cryostat for measurements at 80 K with a 0.07 T applied magnetic field. Isomer shifts were determined relative to α-Fe at 298 K. All Mössbauer spectra were fit using the program WMoss (SeeCo).

Computational Details. Singlet-point calculations on $[(cyIDep)_2Fe]^{1+}$ and $[(sIDep)_2Fe]^{1+}$ were performed with the ORCA 2.8 program[38] using the B3LYP[39] method. The SVP basis set[40] was used for the C, N, and H atoms, and the TZVP basis set[41] was used for the Fe atom. The RIJCOSX approximation[42] with matching auxiliary basis sets[40,43] was employed to accelerate the calculation. TIGHTSCF was used for SCF calculation.[44] The single-point calculations at different spin states (S = 1/2 and 3/2) were based on the coordinates obtained from X-ray diffraction study with optimization on hydrogen atoms only. For the xyz files, please see Supporting Information.

Preparation of cyIDep·HBF_4. The preparation of the imidazolium salt adopts a modified synthetic procedure described by Glorius for cyIMes·HBr.[45] *N*,*N*′-bis(2,6-diethylphenyl)formamidine[46] (11.6 g, 38 mmol, 1.0 equiv) was suspended in acetonitrile (200 mL). $NEt(^iPr)_2$ (5.83 g, 45 mmol, 1.2 equiv) and 2-bromocyclohexanone (13.3 g, 75 mmol, 2.0 equiv) were added successively, and the resulting mixture was stirred at 110 °C for 21 h. Then, the volatiles were removed under reduced pressure. The residue was suspended in toluene (200 mL), to which acetic anhydride (11.5 g, 0.11 mol, 3.0 equiv) and 48% aqueous HBF_4 (10.3 g, 56 mmol, 1.5 equiv) were added. The resulting mixture was stirred at 90 °C for 14 h. The mixture was then transferred into a separatory funnel containing CH_2Cl_2/H_2O (400 mL, 1/1 v/v). After separation of the two layers, the aqueous layer was extracted with CH_2Cl_2 (3 × 100 mL), and then the combined organic layers were washed with distilled water (3 × 100 mL) and dried over anhydrous magnesium sulfate. The volatiles were removed under vacuum to afford oily brown solid. The oily brown solid was washed with Et_2O (3 × 20 mL) and cold THF (20 mL) to afford cyIDep·HBF_4 as a white solid (10.5 g, 59%). ^{1}H NMR (400 MHz, CD_3CN, 22 °C): δ (ppm) 8.72 (s, 1H, NC*H*N), 7.60 (t, J = 7.6 Hz, 2H, *p*-Ar-*H*), 7.43 (d, J = 7.6 Hz, 4H, *m*-Ar-*H*), 2.47 (m, 4H, CH_3CHH), 2.34 (m, 8H, CH_3CHH + $CH_2(CH_2)_2CH_2$), 1.90 (m, 4H, $CH_2(CH_2)_2CH_2$), 1.18 (t, J = 7.6 Hz, 12H, CH_3). ^{13}C NMR (101 MHz, CD_3CN, 21 °C): δ (ppm) 141.97, 135.65, 133.12, 132.74, 130.65, 128.51, 24.72, 21.98, 20.64, 15.15. ^{19}F NMR (376 MHz, CD_3CN, 21 °C): δ (ppm) −150.96 (1F), −151.01(3F). The presence of two ^{19}F NMR signals might be caused by the hydrogen bonding of NCH···F−BF_3. MS (ESI): m/z [M-BF_4^-] calcd. for $C_{27}H_{35}N_2^+$: 387.2795, found: 387.2810.

Preparation of cyIDep. To a white suspension of cyIDep·HBF_4 (22.8 g, 48 mmol, 1.0 equiv) in THF (150 mL) was added KO^{t}Bu (10.8 g, 96 mmol, 2.0 equiv) slowly at room temperature. The color of the mixture turned from white to pale yellow within several minutes. The pale yellow suspension was stirred for 11 h and then filtered through diatomaceous earth to afford pale yellow solution. After removal of the volatiles, the residue was extracted with toluene (100 mL) and filtered to afford pale yellow solution. After further removal of the solvent, the residue was washed with cold *n*-hexane (10 mL) rapidly and dried under vacuum to afford cyIDep as a white solid (17.0 g, 91%). ^{1}H NMR (400 MHz, C_6D_6, 22 °C): δ (ppm) 7.22 (t, J = 7.6 Hz, 2H, *p*-Ar-*H*), 7.12 (d, J = 7.6 Hz, 4H, *m*-Ar-*H*), 2.55 (m, 8H, CH_2CH_3), 2.02 (brs, 4H, $CH_2(CH_2)_2CH_2$), 1.38 (brs, 4H, $CH_2(CH_2)_2CH_2$), 1.22 (t, J = 7.6 Hz, 12H, CH_3). ^{13}C NMR (101 MHz, C_6D_6, 22 °C): δ (ppm) 217.26 (carbene carbon), 142.32, 138.78, 128.44, 127.27, 126.94, 25.30, 23.01, 21.55, 15.35. Anal. Calcd for $C_{27}H_{34}N_2$: C, 83.89; H, 8.87; N, 7.25. Found: C, 83.76; H, 8.92; N, 7.14%.

Preparation of sIDep·HBr.[47] The preparation of the imidazolium salt adopts a modified synthetic procedure described by Nechaev[48] for the preparation of sIPr·HBr. *N*,*N*′-bis(2,6-diethylphenyl)formamidine (34.4 g, 0.11 mol, 1.0 equiv) was suspended in toluene (15 mL). $BrCH_2CH_2Br$ (31.4 g, 0.17 mol, 1.5 equiv) and $NEt(^iPr)_2$ (17.4 g, 0.13 mol, 1.2 equiv) were added successively to the mixture. The resulting

DOI: 10.1021/acs.inorgchem.5b01522
Inorg. Chem. 2015, 54, 8808−8816

mixture was stirred rigorously at 120 °C for 6 h. After it cooled to room temperature, the solid was dissolved in CH_2Cl_2 (250 mL) and washed with diluted solutions of potassium carbonate (3 × 100 mL). The organic layer was separated, dried over anhydrous magnesium sulfate, and filtered. After removal of the volatiles, the remaining residue was then washed with Et_2O and dried under vacuum to afford sIDep·HBr as a pale pink solid (42.5 g, 92%). ^{1}H NMR (300 MHz, CD_3CN, 29 °C): δ (ppm) 9.07 (s, 1H, NC*H*N), 7.48 (t, J = 7.6 Hz, 2H, *p*-Ar-*H*), 7.34 (d, J = 7.6 Hz, 4H, *m*-Ar-*H*), 4.49 (s, 4H, NCH_2), 2.77 (q, J = 7.5 Hz, 8H, CH_3CH_2), 1.31 (t, J = 7.5 Hz, 12H, CH_3CH_2). ^{13}C NMR (75 MHz, CD_3CN, 29 °C): δ (ppm) 160.70, 142.60, 132.48, 131.58, 128.08, 53.59, 24.71, 15.49.

Preparation of sIDep. To a white suspension of sIDep·HBr (36.0 g, 87 mmol, 1.0 equiv) in THF (150 mL) was added potassium bis(trimethylsilyl)amide (1 M in THF, 87 mL, 87 mmol, 1.0 equiv) at −116 °C. After it was stirred for 30 min, the mixture was warmed to room temperature and further stirred for 3 h. The resulting mixture was filtered through diatomaceous earth to afford pale yellow solution. After removal of the volatiles, the residue was extracted with Et_2O (200 mL), filtered through diatomaceous earth to afford a pale yellow solution. Removal of the volatiles gave a yellow residue, which was washed with cold *n*-hexane (15 mL) rapidly and dried in vacuo to afford sIDep as a white crystalline solid (17.3 g, 60%). ^{1}H NMR (300 MHz, C_6D_6, 29 °C): δ (ppm) 7.16 (t, J = 7.2 Hz, 2H, *p*-Ar-*H*), 7.07 (d, J = 7.6 Hz, 4H, *m*-Ar-*H*), 3.31 (s, 4H, CH_2CH_2), 2.69 (q, J = 7.5 Hz, 4H, CH_3CHH), 2.60 (q, J = 7.5 Hz, 4H, CH_3CHH), 1.25 (t, J = 7.5 Hz, 12H, CH_3CH_2). ^{13}C NMR (75 MHz, C_6D_6, 29 °C): δ (ppm) 243.09 (carbene carbon), 142.87, 140.92, 127.75, 127.10, 52.46, 25.20, 15.93. Anal. Calcd for $C_{23}H_{30}N_2$: C, 82.59; H, 9.04; N, 8.37. Found: C, 82.65; H, 9.09; N, 8.45%.

Preparation of [(cyIDep)$_2$FeBr] (1). To a pale yellow suspension of $FeBr_2$ (1.12 g, 5.2 mmol, 1.0 equiv) in THF (35 mL) was added cyIDep (4.00 g, 10 mmol, 2.0 equiv). The mixture was stirred rigorously overnight. After removal of the volatiles, toluene (35 mL) was added to afford a pale brown suspension. The addition of potassium graphite (1.78 g, 13 mmol, 2.5 equiv) to the mixture at room temperature led to quick color change to deep brown. The mixture was stirred for 55 min, and then filtered through diatomaceous earth to afford a brown solution. After removal of the volatiles, the residue was washed with *n*-hexane (50 mL) and dried in vacuo to afford **1** as a brown solid (3.00 g, 64%). Single crystals of **1** suitable for X-ray diffraction studies were grown from its toluene/*n*-hexane solution at −25 °C. The ^{1}H NMR spectrum of this paramagnetic complex displayed six characteristic peaks in the range from −13.61 to 8.76 ppm. ^{1}H NMR (300 MHz, C_6D_6, 22 °C): δ (ppm) 8.76, 5.49, 5.09, 0.10, −8.75, −13.61. Anal. Calcd for $C_{54}H_{68}BrFeN_4$: C, 71.36; H, 7.54; N, 6.16. Found: C, 71.09; H, 7.44; N, 6.18%. Because of the instability of the complex in solution, no further characterization data were acquired.

Preparation of [(sIDep)$_2$FeBr] (2). To a pale yellow suspension of $FeBr_2$ (322 mg, 1.5 mmol, 1.0 equiv) in THF (20 mL) was added sIDep (1.00 g, 3.0 mmol, 2.0 equiv). The reaction was stirred rigorously for 3 h. After removal of the volatiles, toluene (20 mL) was added to the residue to afford a pale brown suspension. One hour later, potassium graphite (504 mg, 3.7 mmol, 2.5 equiv) was added to the pale brown suspension at room temperature. The color of the mixture turned to purple. After it was stirred for 15 min, the mixture was filtered through diatomaceous earth to afford a purple solution. Removal of the volatiles gave a purple residue, which was washed with *n*-hexane (15 mL) and dried in vacuo to afford **2** as a pale purple solid (980 mg, 82%). Single crystals of **2** suitable for X-ray diffraction studies were grown from its toluene/hexane solution at −25 °C. The ^{1}H NMR spectrum of this paramagnetic complex displayed five characteristic peaks in the range from −34.48 to 11.18 ppm. ^{1}H NMR (400 MHz, C_6D_6, 22 °C): δ (ppm) 11.18, 4.01, −7.95, −12.11, −34.48. Anal. Calcd for $C_{46}H_{60}BrFeN_4$: C, 68.65; H, 7.51; N, 6.96. Found: C, 68.25; H, 7.59; N, 6.79%. Because of the instability of the complex in solution, no further characterization data were acquired.

Preparation of [(cyIDep)$_2$Fe][BAr$^F_4$] (3). To a brown suspension of **1** (1.00 g, 1.1 mmol, 1.0 equiv) in Et_2O (15 mL) was added $NaBAr^F_4$ (sodium tetra(3,5-di(trifluoromethyl)phenyl)borate, 975 mg, 1.1 mmol, 1.0 equiv). The color of the mixture quickly turned to bright red. After it was stirred for 30 min, the mixture was filtered through diatomaceous earth. The solution was concentrated under vacuum to afford a red residue, which was washed with *n*-hexane (20 mL) and then dissolved in Et_2O (25 mL). After the red solution was allowed to stand at −25 °C for two days to facilitate crystallization, **3** was afforded as a red purple crystalline solid (1.48 g, 80%). The ^{1}H NMR spectrum of this paramagnetic complex displayed eight characteristic peaks in the range from −10.83 to 20.67 ppm, which remained almost unchanged for 7 d in THF-d_8 at room temperature. ^{1}H NMR (400 MHz, THF-d_8, 22 °C): δ (ppm) 20.67, 17.94, 15.53, 7.87, 7.64, 4.00, 3.52, −10.83. Magnetic susceptibility (THF-d_8): μ_{eff} = 5.5(2) μ_B. Absorption spectrum (THF): $\lambda_{max,\ nm}$ (ε, M^{-1} cm^{-1}) = 340 (3180), 428 (3710), 491 (3680), 541 (4850), 746 (40), 835 (70), 1310 (110), 1419 (70). Anal. Calcd for $C_{86}H_{80}BF_{24}FeN_4$: C, 61.04; H, 4.77; N, 3.31. Found: C, 60.88; H, 4.79; N, 3.15%.

Preparation of [(sIDep)$_2$Fe][BAr$^F_4$] (4). To a purple suspension of **2** (1.00 g, 1.2 mmol, 1.0 equiv) in Et_2O (15 mL) was added $NaBAr^F_4$ (1.10 g, 1.2 mmol, 1.0 equiv). The color of the mixture turned to orange quickly. The mixture was stirred for 30 min and then filtered through diatomaceous earth to afford an orange solution. After removal of the solvent, the residue was washed with Et_2O/*n*-hexane (10 mL, 3/1) and then dissolved in Et_2O/*n*-hexane (25 mL, 10/1). After the orange-red solution was allowed to stand at −25 °C for 3 d to facilitate crystallization, **4** was afforded as an orange crystalline solid (1.28 g, 65%). The ^{1}H NMR spectrum of this paramagnetic complex displayed seven characteristic peaks in the range from −78.38 to 21.70 ppm, which changed slowly after 1 d in THF-d_8 at room temperature. ^{1}H NMR (400 MHz, THF-d_8, 22 °C): δ (ppm) 21.70, 18.65, 7.87, 7.62, 4.41, 3.19, −78.38. The ^{1}H NMR spectrum should correspond to the mixture of [(sIDep)$_2$Fe][BAr$^F_4$] and [(sIDep)$_2$Fe(THF)][BAr$^F_4$]. Absorption spectrum (Et_2O): $\lambda_{max,\ nm}$ (ε, M^{-1} cm^{-1}) = 343 (2270), 432 (2820), 470 (4090), 503 (3720), 706 (60), 791 (40), 1192 (70), 1352 (40). Anal. Calcd for $C_{78}H_{72}BF_{24}FeN_4$: C, 58.99; H, 4.57; N, 3.53. Found: C, 59.34; H, 4.98; N, 3.58%.

Preparation of [(sIMes)$_2$Fe(THF)][BPh$_4$]·Et$_2$O (5·Et$_2$O). To a pale green suspension of $[Fe(tmeda)Cl_2]_2$ (595 mg, 1.2 mmol, 1.0 equiv) in THF (20 mL) was added sIMes[49] (1.50 g, 4.9 mmol, 4.0 equiv). The mixture was stirred for 2 h. After removal of the volatiles, THF (20 mL) was added to the residue to afford a pale yellow suspension. 0.5 h later, potassium graphite (993 mg, 7.3 mmol, 6.0 equiv) was added to the pale yellow suspension at room temperature. The color of the mixture turned red-purple. The mixture was stirred for 4 min and then quickly filtered through diatomaceous earth to afford a red-purple solution. $NaBPh_4$ (838 mg, 2.5 mmol, 2.0 equiv) was added to the solution immediately. The mixture was stirred for 30 min and then filtered through diatomaceous earth to afford an orange-red solution. After removal of the volatiles, the residue was washed sequentially with *n*-hexane (20 mL) and Et_2O (20 mL) and then dissolved in THF/Et_2O (25 mL, 4/1) to afford an orange-red solution. After the solution was allowed to stand at −25 °C for several days to facilitate recrystallization, **5**·Et_2O was obtained as a red crystalline solid (1.21 g, 44%). The ^{1}H NMR spectrum of this paramagnetic complex displayed six characteristic peaks in the range from −71.26 to 7.97 ppm, which remained almost unchanged for at least 7 d in THF-d_8 at room temperature. ^{1}H NMR (400 MHz, THF-d_8, 22 °C): δ (ppm) 7.97, 6.88, 6.62, 2.47, 1.88, −71.26. Magnetic susceptibility (THF-d_8): μ_{eff} = 4.7(2) μ_B. Absorption spectrum (THF): $\lambda_{max,\ nm}$ (ε, M^{-1} cm^{-1}) = 346 (3620), 489 (6410), 796 (90), 1060 (110), 1386 (160). Anal. Calcd for $C_{74}H_{90}BFeN_4O_2$: C, 78.36; H, 8.00; N, 4.94. Found: C, 78.43; H, 7.77; N, 4.94%.

■ ASSOCIATED CONTENT

Supporting Information

The Supporting Information is available free of charge on the ACS Publications website at DOI: 10.1021/acs.inorgchem.5b01522.

DOI: 10.1021/acs.inorgchem.5b01522
Inorg. Chem. 2015, 54, 8808−8816

Table of crystal data and collection parameters, tabulated computed relative free energies, ^{57}Fe Mössbauer spectra, absorption spectra, cyclic voltammograms, photographs of the THF solutions, and NMR spectra. (PDF)
X-ray crystallographic information for five compounds. (CIF)
Cartesian coordinates for the computed structures. (XYZ)

AUTHOR INFORMATION

Corresponding Author

*E-mail: deng@sioc.ac.cn.

Notes

The authors declare no competing financial interest.

ACKNOWLEDGMENTS

The work was supported by the National Basic Research Program of China (No. 2011CB808705 to L.D.), the National Natural Science Foundation of China (Nos. 21222208, 21421091, and 21432001 to L.D.), and a grant from the National Institutes of Health (No. R01GM111480 to M.L.N.).

REFERENCES

(1) Twigg, M. V.; Burgess, J. In *Comprehensive Coordination Chemistry II;* McCleverty, J. A.; Meyer, T. J., Eds.; Elsevier: Amsterdam, The Netherlands, 2005; Vol. *5*, p 460.

(2) For reviews on low-coordinate iron(III) and iron(II) compounds, see: (a) Bradley, D. C.; Chisholm, M. H. *Acc. Chem. Res.* **1976**, *9*, 273. (b) Cummins, C. C. *Progress in Inorganic Chemistry* **1998**, *47*, 685. (c) Holland, P. L. *Acc. Chem. Res.* **2008**, *41*, 905. (d) Power, P. P. *Chem. Rev.* **2012**, *112*, 3482.

(3) For examples, see: (a) Rodriguez, M. M.; Bill, E.; Brennessel, W. W.; Holland, P. L. *Science* **2011**, *334*, 780. (b) Anderson, J. S.; Rittle, J.; Peters, J. C. *Nature* **2013**, *501*, 84.

(4) For a recent review, please see: Craig, G. A.; Murrie, M. *Chem. Soc. Rev.* **2015**, *44*, 2135.

(5) Chiang, K. P.; Scarborough, C. C.; Horitani, M.; Lees, N. S.; Ding, K.; Dugan, T. R.; Brennessel, W. W.; Bill, E.; Hoffman, B. M.; Holland, P. L. *Angew. Chem., Int. Ed.* **2012**, *51*, 3658.

(6) Rodriguez, M. M.; Stubbert, B. D.; Scarborough, C. C.; Brennessel, W. W.; Bill, E.; Holland, P. L. *Angew. Chem., Int. Ed.* **2012**, *51*, 8247.

(7) Yu, Y.; Smith, J. M.; Flaschenriem, C. J.; Holland, P. L. *Inorg. Chem.* **2006**, *45*, 5742.

(8) Smith, J. M.; Sadique, A. R.; Cundari, T. R.; Rodgers, K. R.; Lukat-Rodgers, G.; Lachicotte, R. J.; Flaschenriem, C. J.; Vela, J.; Holland, P. L. *J. Am. Chem. Soc.* **2006**, *128*, 756.

(9) Ingleson, M. J.; Fullmer, B. C.; Buschhorn, D. T.; Fan, H.; Pink, M.; Huffman, J. C.; Caulton, K. G. *Inorg. Chem.* **2008**, *47*, 407.

(10) Fohlmeister, L.; Liu, S.; Schulten, C.; Moubaraki, B.; Stasch, A.; Cashion, J. D.; Murray, K. S.; Gagliardi, L.; Jones, C. *Angew. Chem., Int. Ed.* **2012**, *51*, 8294.

(11) Zadrozny, J. M.; Xiao, D. J.; Atanasov, M.; Long, G. J.; Grandjean, F.; Neese, F.; Long, J. R. *Nat. Chem.* **2013**, *5*, 577.

(12) Ung, G.; Rittle, J.; Soleilhavoup, M.; Bertrand, G.; Peters, J. C. *Angew. Chem., Int. Ed.* **2014**, *53*, 8427.

(13) Samuel, P. P.; Mondal, K. C.; Amin Sk, N.; Roesky, H. W.; Carl, E.; Neufeld, R.; Stalke, D.; Demeshko, S.; Meyer, F.; Ungur, L.; Chibotaru, L. F.; Christian, J.; Ramachandran, V.; van Tol, J.; Dalal, N. S. *J. Am. Chem. Soc.* **2014**, *136*, 11964.

(14) Mo, Z.; Ouyang, Z.; Wang, L.; Fillman, K. L.; Neidig, M. L.; Deng, L. *Org. Chem. Front.* **2014**, *1*, 1040.

(15) Lin, C.-Y.; Fettinger, J. C.; Grandjean, F.; Long, G. J.; Power, P. P. *Inorg. Chem.* **2014**, *53*, 9400.

(16) Werncke, C. G.; Bunting, P. C.; Duhayon, C.; Long, J. R.; Bontemps, S.; Sabo-Etienne, S. *Angew. Chem., Int. Ed.* **2015**, *54*, 245.

(17) Lipschutz, M. I.; Chantarojsiri, T.; Dong, Y.; Tilley, T. D. *J. Am. Chem. Soc.* **2015**, *137*, 6366.

(18) (a) Lavallo, V.; Canac, Y.; Prasang, C.; Donnadieu, B.; Bertrand, G. *Angew. Chem., Int. Ed.* **2005**, *44*, 5705. (b) Hahn, F. E.; Jahnke, M. C. *Angew. Chem., Int. Ed.* **2008**, *47*, 3122.

(19) For reference on the π-acidity of NHC ligands, see: (a) Liske, A.; Verlinden, K.; Buhl, H.; Schaper, K.; Ganter, C. *Organometallics* **2013**, *32*, 5269. (b) Back, O.; Henry-Ellinger, M.; Martin, C. D.; Martin, D.; Bertrand, G. *Angew. Chem., Int. Ed.* **2013**, *52*, 2939. (c) Jacobsen, H.; Correa, A.; Poater, A.; Costabile, C.; Cavallo, L. *Coord. Chem. Rev.* **2009**, *253*, 687. (d) Fillman, K. L.; Przyojski, J. A.; Al-Afyouni, M. H.; Tonzetich, Z. J.; Neidig, M. L. *Chem. Sci.* **2015**, *6*, 1178.

(20) (a) Xiang, L.; Xiao, J.; Deng, L. *Organometallics* **2011**, *30*, 2018. (b) Danopoulos, A. A.; Braunstein, P.; Stylianides, N.; Wesolek, M. *Organometallics* **2011**, *30*, 6514. (c) Day, B. M.; Pugh, T.; Hendriks, D.; Guerra, C. F.; Evans, D. J.; Bickelhaupt, F. M.; Layfield, R. A. *J. Am. Chem. Soc.* **2013**, *135*, 13338.

(21) Zhang, H.; Ouyang, Z.; Liu, Y.; Zhang, Q.; Wang, L.; Deng, L. *Angew. Chem., Int. Ed.* **2014**, *53*, 8432.

(22) (a) Miyazaki, S.; Koga, Y.; Matsumoto, T.; Matsubara, K. *Chem. Commun.* **2010**, *46*, 1932. (b) Lee, C. H.; Cook, T. R.; Nocera, D. G. *Inorg. Chem.* **2011**, *50*, 714. (c) Zhang, K.; Conda-Sheridan, M.; Cooke, S. R.; Louie, J. *Organometallics* **2011**, *30*, 2546.

(23) Poulten, R. C.; Page, M. J.; Algarra, A. G.; Le Roy, J. J.; López, I.; Carter, E.; Llobet, A.; Macgregor, S. A.; Mahon, M. F.; Murphy, D. M.; Murugesu, M.; Whittlesey, M. K. *J. Am. Chem. Soc.* **2013**, *135*, 13640.

(24) Altenhoff, G.; Goddard, R.; Lehmann, C. W.; Glorius, F. *Angew. Chem., Int. Ed.* **2003**, *42*, 3690.

(25) Fortman, G. C.; Scott, N. M.; Linden, A.; Stevens, E. D.; Dorta, R.; Nolan, S. P. *Chem. Commun.* **2010**, *46*, 1050.

(26) Díez-González, S.; Stevens, E. D.; Scott, N. M.; Petersen, J. L.; Nolan, S. P. *Chem. - Eur. J.* **2008**, *14*, 158.

(27) Arduengo, A. J.; Dias, H. V. R.; Calabrese, J. C.; Davidson, F. *Organometallics* **1993**, *12*, 3405.

(28) Gaillard, S.; Nun, P.; Slawin, A. M. Z.; Nolan, S. P. *Organometallics* **2010**, *29*, 5402.

(29) Mo, Z.; Chen, D.; Leng, X.; Deng, L. *Organometallics* **2012**, *31*, 7040.

(30) (a) Hendrich, M. P.; Gunderson, W.; Behan, R. K.; Green, M. T.; Mehn, M. P.; Betley, T. A.; Lu, C. C.; Peters, J. C. *Proc. Natl. Acad. Sci. U. S. A.* **2006**, *103*, 17107. (b) Vogel, C.; Heinemann, F. W.; Sutter, J.; Anthon, C.; Meyer, K. *Angew. Chem., Int. Ed.* **2008**, *47*, 2681. (c) Scepaniak, J. J.; Vogel, C. S.; Khusniyarov, M. M.; Heinemann, F. W.; Meyer, K.; Smith, J. M. *Science* **2011**, *331*, 1049. (d) Rudd, P. A.; Liu, S.; Planas, N.; Bill, E.; Gagliardi, L.; Lu, C. C. *Angew. Chem., Int. Ed.* **2013**, *52*, 4449.

(31) Hohenberger, J.; Ray, K.; Meyer, K. *Nat. Commun.* **2012**, *3*, 720.

(32) Stoian, S. A.; Yu, Y.; Smith, J. M.; Holland, P. L.; Bominaar, E. L.; Münck, E. *Inorg. Chem.* **2005**, *44*, 4915.

(33) Fisher, K. J.; Bradley, D. C. *J. Am. Chem. Soc.* **1971**, *93*, 2058.

(34) Gregory, E. A.; Lachicotte, R. J.; Holland, P. L. *Organometallics* **2005**, *24*, 1803.

(35) (a) Evans, D. F. *J. Chem. Soc.* **1959**, 2003. (b) Sur, S. K. *J. Magn. Reson.* **1989**, *82*, 169.

(36) Sheldrick, G. M. *SADABS,* Program for Empirical Absorption Correction of Area Detector Data; University of Göttingen: Germany, 1996.

(37) Sheldrick, G. M. *SHELXTL 5.10 for Windows NT: Structure Determination Software Programs;* Bruker Analytical X-ray systems, Inc.: Madison, WI, 1997.

(38) Neese, F. *ORCA,* An Ab Initio, Density Functional, and Semiempirical Program Package (v. 2.8); Universität Bonn: Germany, 2011.

(39) (a) Becke, A. D. *J. Chem. Phys.* **1993**, *98*, 5648. (b) Lee, C.; Yang, W.; Parr, R. G. *Phys. Rev. B: Condens. Matter Mater. Phys.* **1988**, *37*, 785.

(40) Schaefer, A.; Horn, H.; Ahlrichs, R. *J. Chem. Phys.* **1992**, *97*, 2571.

DOI: 10.1021/acs.inorgchem.5b01522
Inorg. Chem. 2015, 54, 8808−8816

(41) Schaefer, A.; Huber, C.; Ahlrichs, R. *J. Chem. Phys.* **1994**, *100*, 5829.
(42) Neese, F.; Wennmohs, F.; Hansen, A.; Becker, U. *Chem. Phys.* **2009**, *356*, 98.
(43) Weigend, F.; Ahlrichs, R. *Phys. Chem. Chem. Phys.* **2005**, *7*, 3297.
(44) *Manual for ORCA,* Version 2.8; Universität Bonn: Germany, 2010; p 453.
(45) Hirano, K.; Urban, S.; Wang, C.; Glorius, F. *Org. Lett.* **2009**, *11*, 1019.
(46) Ueda, N.; Nikawa, H.; Takano, Y.; Ishitsuka, M. O.; Tsuchiya, T.; Akasaka, T. *Heteroat. Chem.* **2011**, *22*, 426.
(47) Hadei, N.; Kantchev, E. A. B.; O'Brien, C. J.; Organ, M. G. *J. Org. Chem.* **2005**, *70*, 8503.
(48) Kolychev, E. L.; Asachenko, A. F.; Dzhevakov, P. B.; Bush, A. A.; Shuntikov, V. V.; Khrustalev, V. N.; Nechaev, M. S. *Dalton Trans.* **2013**, *42*, 6859.
(49) Iglesias, M.; Beetstra, D. J.; Knight, J. C.; Ooi, L.-L.; Stasch, A.; Coles, S.; Male, L.; Hursthouse, M. B.; Cavell, K. J.; Dervisi, A.; Fallis, I. A. *Organometallics* **2008**, *27*, 3279.

DOI: 10.1021/acs.inorgchem.5b01522
Inorg. Chem. 2015, 54, 8808−8816